Ann. Occup. Hyg., 2016, Vol. 60, No. 2, 220–230
doi:10.1093/annhyg/mev066
Advance Access publication 21 September 2015

The Chartered Society for Worker Health Protection

On the Characterization of the Generation Rate and Size-Dependent Crystalline Silica Content of the Dust from Cutting Fiber Cement Siding

Chaolong Qi*, Alan Echt and Michael G. Gressel

Centers for Disease Control and Prevention, National Institute for Occupational Safety and Health, 1090 Tusculum Ave, MS R5, Cincinnati, OH 45226, USA
*Author to whom correspondence should be addressed. Tel: (513) 841-4532; fax: (513) 841-4545; e-mail: hif1@cdc.gov
Submitted 27 May 2015; revised 8 July 2015; revised version accepted 8 August 2015.

ABSTRACT

A laboratory testing system was developed to systematically characterize the dust generation rate and size-dependent crystalline silica content when cutting or shaping silica containing materials. The tests of cutting fiber cement siding in this system verify that it provides high test repeatability, making it suitable for the targeted characterizations. The mass-based size distributions obtained from a gravimetric-based instrument and a direct reading instrument both show bimodal lognormal distributions with a larger mode ~13 μm and another mode <5 μm for the dusts from cutting four different brands of fiber cement siding. The generation rates of respirable dust obtained from the two instruments are comparable, and the results from each instrument are similar for the four brands. The silica content in the airborne dusts, however, strongly depends on the amount of silica used in the respective product. It is also observed that the silica content in the airborne dust from cutting the four brands of fiber cement siding showed the same trend of an increase with the aerodynamic diameter of the dust, approaching the silica content levels found in their respective bulk samples. Combining the results for both the dust size distribution and size-dependent silica content, it is found that most of the respirable crystalline silica (RCS) resides in the dust ~2.5 μm in aerodynamic diameter. These results would help guide the development of specific engineering control measures targeted at lowering workers' exposure to RCS while cutting fiber cement siding. With the high repeatability using the laboratory testing system, the dust generation rate could then be characterized under different operating conditions, and with the deployment of various engineering control measures. This would greatly facilitate the systematic evaluation of the control effectiveness and the selection of the optimal control solutions for field trials.

KEYWORDS: crystalline silica; dust generation; fiber cement; MOUDI

INTRODUCTION

Respirable crystalline silica (RCS) refers to the portion of airborne crystalline silica dust that is capable of entering the gas-exchange regions of the lungs if inhaled (NIOSH, 2002). The three major forms of crystalline silica are quartz, cristobalite, and tridymite; quartz is the most common form (Bureau of Mines, 1992). Silicosis, a fibrotic disease of the lungs, is an occupational respiratory disease caused by the inhalation and deposition of RCS (NIOSH, 1986).

Fiber cement is a construction material often used as siding in place of wood or vinyl. Cellulose fiber, silica sand, cement, and water are the principal ingredients used in the manufacture of fiber cement products. Power saws, such as circular saws and compound miter saws, are commonly used to cut fiber cement siding. The study by Lofgren *et al.* (2004) reported that fiber cement board cutters' uncontrolled exposures to RCS ranged from 0.02 milligrams per cubic meter (mg m^{-3}) to 0.27 mg m^{-3} during sampling, and 8-h time weighted average (TWA) exposure ranged from 0.01 to 0.17 mg m^{-3}. The highest result was 3.4 times the NIOSH recommended exposure limit (REL) for RCS of 0.05 mg m^{-3}. In an in-depth field survey, Qi *et al.* (2013) reported a cutter's uncontrolled exposures to RCS ranged from 0.06 to 0.13 mg m^{-3} during sampling, and 8-h TWA exposure ranged from 0.02 to 0.13 mg m^{-3}. The highest result was 2.6 times the NIOSH REL for RCS. The data from both field surveys suggested excessive exposures to RCS occurred when no engineering control was used for cutting fiber cement siding. In addition, the market share of fiber cement siding has climbed from 1 to 13% from 1991 to 2010 (US Census Bureau, 2013), and is expected to continue to increase. The number of workers exposed to dust containing crystalline silica as a result can also be expected to increase as the use of fiber cement siding displaces other siding products. The excessive exposures and increasing workforce suggest the need for engineering control measures to consistently prevent overexposures to RCS while cutting fiber cement siding.

For any process that generates RCS, knowing the dust generation rate, the dust size distribution, and the silica content in the dust of different sizes would guide the development of effective and economical engineering control solutions. However, many dust-generating processes have not been fully characterized nor well investigated and documented. Part of the reason can be attributed to the lack of reliable characterization methods and the complex nature of the processes generating RCS. Sirianni *et al.* (2008) used a particle counter with six size channels and three size-selective devices to understand the size distribution and size-related silica content in granite quarry dust. They observed a varying dust size distribution from different tasks, and a small increase of silica content with the size of the sampled dust. None of the devices, however, was capable of providing a quantitative correlation between the silica content and dust size for the studied tasks. Shepherd *et al.* (2009) used four-stage personal cascade impactors and observed a moderate increase in silica content with the size of the dust from concrete cutting. Both studies were based on field experiments, which cannot avoid uncertainties from varying field conditions such as wind, ventilation, or work practices.

This paper describes a laboratory testing system developed to systematically characterize dust generation rate and size-dependent silica content. The system aims to provide high repeatability in a laboratory setting with other conditions well controlled. The characterization results for cutting fiber cement siding are then presented, validating the testing system and this overall approach. These results will help in the development of feasible engineering control measures.

METHODS

Laboratory testing system

Figure 1 illustrates a diagram of the laboratory testing system used in this study. It was designed according to the European Standard EN 1093-3 (CEN, 2006). A dust collection air handling unit (PSKB-1440, ProVent LLC, Harbor Springs, MI, USA) was used as an air mover for the system. The air handling unit was connected to an automatic tool testing chamber through a 0.3 m diameter duct ~6.4 m long. A funnel section connected the duct to the automatic tool testing chamber, which had a square cross section of 1.2 m wide and 1.2 m high. A blast gate upstream of the air handling unit was used to adjust the air flow rate passing through the testing system by allowing the excessive air to enter the air handling unit through the gate. Once turned on, the air handling unit was set to draw room air into the testing system at a flow rate of 0.64 m^3 s^{-1}. This flow rate was set by manually adjusting the blast gate valve and was monitored by a micromanometer (PVM100 Airflow Developments Ltd., UK) connected to a Delta tube (306AM-11-AO, Mid-West Instrument, Sterling, MI, USA). The Delta tube functioned as an averaging pitot tube and has four pressure-averaging ports on the front and backside of a tear-shaped or circular cylinder (Miller, 1989). The accuracy of the flow rate measured by this Delta tube was verified by Heitbrink and Bennett (2006), who compared the flow rate obtained

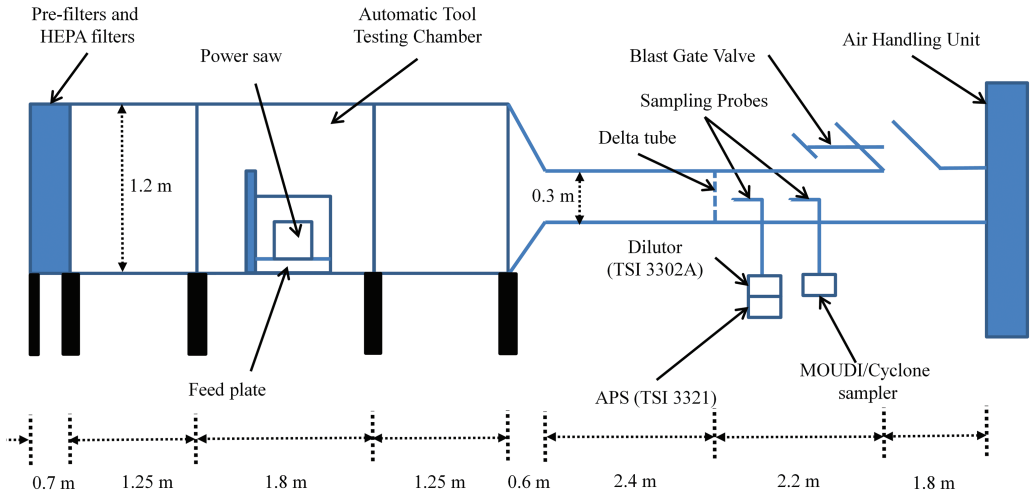

Figure 1 Diagram of the laboratory testing system.

from the Delta tube (Mid-West Instrument, 2004) and that measured using a 10-point pitot tube traverse of the duct performed in the horizontal and vertical planes (~0.8% difference). Two aerosol sampling ports were open on the duct for mounting the sampling probes of all the sampling instruments used in this study. These two ports and the Delta tube formed the sampling section of the system. The location of this sampling section on the duct was designed to meet the requirement of European Standard EN 1093-3 (CEN, 2006) for taking representative samples of respirable dust, and it was verified through experiment in this study (see the Supplementary Data).

The air flow that entered the system first passed through a filter panel, which had the same cross section as the automatic tool testing chamber and was 0.7 m long. The filter panel included one bank of four pre-filters and another bank of four high-efficiency particulate air filters that removed most the particles in the room air so that they did not interfere with the analysis of the dust generated inside the testing system. The filters also helped ensure that the air that entered the system had a uniform velocity profile across the panel's cross section. After the filtration section was the automatic tool testing chamber, which was 4.3 m long and was specifically designed and constructed for the cutting of fiber cement siding. The air handling unit collected the dust generated in the testing system with two filter cartridges (P25.20, ProVent LLC, Harbor Springs, MI, USA) before the cleaned air was discharged back into the room.

The walls of the automatic tool testing chamber were transparent, so the operation inside could be visually observed. The chamber featured automatic control using programmable logic controller (PLC) and human machine interface (HMI). A compound miter saw (Model C12LSH, Hitachi Power Tools, Valencia, CA, USA) with an eight-tooth polycrystalline diamond tipped (PCD) blade (Model 18109, Hitachi Power Tools) was used to make all the cuts for this study. The saw was mounted in the chamber using a specially designed fixture. The operation was controlled using a two-dimensional actuator through the PLC. One fiber cement siding board was mounted on a chain-driven feed plate, and the feed rate was automatically controlled through the PLC. Board feed rate and saw operation were programmed through the HMI so that automatic and repeatable cuts were achieved. The saw was configured to cut ~9 cm of the board's width by chopping and to cut the rest by sliding. The sliding speed was set at 2.54 cm s^{-1}. Four different brands of fiber cement siding were evaluated in this study. Detailed specifications of these products are listed in Supplementary Table S1.

Sampling methods

In this study, the automatic tool testing chamber was set to make a fixed number of repeat cuts of the fiber cement siding board for each test condition. A Micro-Orifice Uniform Deposition Impactor (MOUDI, Model 110, MSP Corp, Shoreview, MN, USA) sampler was used to collect size-selective filter samples

from one of the two duct sampling ports. An isokinetic sampling probe was designed for the MOUDI with a matching flow velocity for the inlet of the sampling probe and the duct. The sampling probe bent 90° and vertically connected to the MOUDI's inlet. The MOUDI is an inertial cascade impactor with 10 stages. It collects dusts according to their inertia on the substrates of the 10 corresponding impaction plates with the 50% cut point for each plate (D_{50}) ranging from 0.056 to 10.0 μm. D_{50} is the aerodynamic diameter of the particle at which penetration declines to 50% (Vincent, 2007). It has an additional inlet stage with a D_{50} of 18 μm. In this study, 47-mm diameter, 5-μm pore-size polyvinyl chloride (PVC) filters were used as the substrates. A 37-mm diameter, 5-μm pore-size PVC filter was used as the final filter collecting all the residual dust. By pre-weighing and post-weighing the PVC filters, the mass of dust collected on each stage was obtained and a mass-based size distribution of the sampled dust was derived. It should be noted that the size distribution obtained from MOUDI may underestimate for larger particles, which have a higher fraction bouncing off the substrates due to their higher inertial effect. Crystalline silica analysis of the filter samples was also performed using X-ray diffraction (XRD) in accordance with NIOSH Method 7500 (NIOSH, 2003). Thus, the content of crystalline silica in the dust of different sizes was obtained from the MOUDI samples.

Using the same sampling port on the duct of the testing system as MOUDI, a GK4.162 RASCAL cyclone sampler (BGI, Waltham, MA, USA) was used alternatively to take air samples of respirable dust from the duct sampling port on the testing system. A Leland Legacy Sample Pump (SKC Inc., Eighty Four, PA, USA) provided a sampling flow rate of 9.5 l min^{-1} for the cyclone. The pump connected via Tygon® tubing to a pre-weighed, 47-mm diameter, 5-μm pore-size PVC filter supported by a backup pad in a conductive filter cassette sealed with a cellulose shrink band (in accordance with NIOSH Methods 0600 and 7500) (NIOSH, 1998, 2003). The mass of the collected respirable dust on the PVC filters was obtained by post-weighing the filters and subtracting their pre-weights. It offered a direct measurement of the mass of the respirable dust. The performance of the GK4.162 cyclone was characterized experimentally by the Health and Safety Laboratory (2011). At a flow rate of 9.5 l min^{-1}, the cyclone has D_{50} of 3.7 μm. The GK4.162 cyclone conforms to the respirable sampling convention defined in EN481 by Comite´ Europe´en de Normalisation (CEN, 1993), and the International Organization for Standardization document 7708 (ISO, 1995). A sampling probe was designed to provide isokinetic sampling for the cyclone at Q_{Cyc} of 9.5 l min^{-1} by matching flow velocity for its inlet and the duct. The generation rate of respirable dust from the cyclone data (G_{Cyc} with a unit of g m^{-1}) is defined and described as:

$$G_{Cyc} = \frac{M_{res} Q}{n_c n_b W Q_{Cyc}} \quad (1)$$

where, M_{res} is the mass of the respirable dust collected on the filters (unit of gram or g); Q is the volume flow rate in the testing system, 0.64 m^3 s^{-1}; n_c is the number of repeating cut during the cyclone sampling; n_b is the number of board per cut (1 in this study); and W is the board width, as listed in Supplementary Table S1. Because all fiber cement siding boards in this study were cut by making cross cuts across the board width, the product of n_b and W represents the total linear length per cut. The total linear length cut is commonly used in practice to account for cutting productivity.

In addition, an aerodynamic particle spectrometer (APS, Model 3321, TSI Inc., Shoreview, MN, USA) was used in the second sampling port to provide real-time measurement of the size distribution of the dust generated with a 1-s time resolution. The 1-s time resolution allowed the APS to capture the entire dust cloud profile for each individual cut, and avoid overlaps of measurement between two adjacent cuts. An isokinetic sampling probe was also designed for the APS. It was connected to an aerosol dilutor (model 3302A; TSI Inc.), which sat on top of the APS. The dilutor was configured to provide a 100 to 1 dilution so that measurement uncertainty caused by high concentration aerosols was minimized. The APS data have taken into account the dilution ratio and particle loss inside the dilutor. The dust size distribution directly measured by the APS is based on number concentration, and it can be used to derive the mass concentration by assuming the shape and density of the sampled dusts. In this study, the dusts are assumed to be spherical. However, it is not straightforward to obtain the actual dust density as the bulk material of fiber cement siding is a mixture of a few different ingredients, and

the density might vary depending on the size of the dust. Thus, the measured board density listed in Supplementary Table S1 was used as the dust density. With the assumed shape and density for the sampled dusts as well as the respirable fraction from the convention curve, the mass concentration of respirable dusts from the APS data could be calculated. It may be different from the actual value. However, this difference should be consistent among all the APS data and should not affect the comparison of the generation rate of respirable dust derived from the APS data by the following equation:

$$G_{\mathrm{APS}} = \frac{\sum_{t=1}^{T_s}(C_{m,t}Q)}{n_b W} \qquad (2)$$

where, $C_{m,t}$ is the mass concentration of respirable dust from one set of the APS data (1 s); and T_s is the total sampling time of the APS for one cut. The APS data contains one set of dust size distribution for every second during the test, which leads to a $C_{m,t}$ data point for each second. Assuming $C_{m,t}$ is the average concentration across the duct's cross section, the summation of $C_{m,t}Q$ during the sampling time T_s results in the total mass of respirable dust generated for one cut. Thus, the generation rate of respirable dust defined in equation (2) also represents the mass of respirable dust generated per unit linear length cut.

The loss of dust inside the sampling probes can be attributed to the settling loss in the horizontal part of the probe, the inertial loss at the 90° bend, and the diffusion loss throughout the probe. These losses are size dependent, so the overall loss of respirable dust depends on the size distribution of the dust generated during cutting of fiber cement siding. The overall loss of respirable dust was calculated using the equations summarized by Brockmann (2011) and the number-based size distribution data from the APS, and it was found to be <1% combining all three aforementioned losses for all three sampling probes.

Four brands of fiber cement siding were cut under the same testing condition. For each brand, three respirable dust samples were collected by the GK4.162 cyclone sampler with 15–30 repeated cuts for each sample, and three sets of MOUDI samples (30 cuts for each sample) were also collected. APS data corresponding to each sample from the GK4.162 cyclone sampler and the MOUDI were recorded. Detailed operating procedure for the cutting test is documented in the Supplementary Data.

All the air samples from MOUDI and the GK4.162 cyclone were prepared and analyzed in accordance with NIOSH Methods 0600 (NIOSH, 1998). For cutting the fiber cement siding brand, two bulk dust samples were also collected from the dust settled on the floor of the automatic tool testing chamber following NIOSH Method 7500 (NIOSH, 2003). Crystalline silica analysis of the air and bulk samples was performed using XRD according to NIOSH Method 7500 (NIOSH, 2003). The limit of detection (LOD) and limit of quantitation (LOQ) for all the analyzed samples are listed in Supplementary Table S2 with a description on which samples were above the LOD/LOQ (see Supplementary Table S2). Quartz was found to be the only form of crystalline silica in the dust in this study.

Analysis of the APS data from a trial test with 15 cuts under the same testing condition revealed that the relative standard deviation (RSD, the ratio of the standard deviation to the mean) for the G_{APS} calculated from each of the 15 cuts was about only 3.1%, demonstrating excellent repeatability of the test. With the high repeatability, three or more repeated cuts under the same testing condition were considered sufficient to provide statistically reliable results. Additional trial tests found that 15–30 cuts were optimal to collect sufficient respirable dust in the cyclone sampler without overloading the filter (2.0 mg/sample, NIOSH, 1998). The RSD for the three replicates of G_{Cyc} was below 3.7% for cutting the four brands of siding. The small RSD for the data from both APS and the cyclone sampler confirms that the laboratory testing system is capable of providing high repeatability, making it suitable for the targeted characterizations. For each MOUDI test, a trial test found that 30 cuts were optimal to ensure that each stage collected dust above the LOD (90 μg/sample, see Supplementary Table S2) and below the overloading level.

RESULTS AND DISCUSSIONS

Size distribution of the dust from cutting fiber cement siding

Figure 2 shows typical size distributions of the dust generated and observed in this study. The size

distributions represent the dust concentration (number or mass) per unit width of size channel on a log scale at different aerodynamic diameters. The MOUDI data were obtained by using the following equation:

$$\frac{dM}{d\log(d_p)} = \frac{m_i}{Q_M T_M \Delta\log(d_p)} \quad (3)$$

where, m_i is the mass of the dust collected on the filter of stage i of the MOUDI; Q_M is the sampling flow rate of the MOUDI (30 l min^{-1}); T_M is the total sampling time of the MOUDI for one test; and $\Delta\log(d_p)$ is the width of the size channel on a log scale for the MOUDI. Following Marple *et al.* (1991), it is assumed that the inlet stage has an upper size limit of 100 μm, and the final filter stage has a lower size limit of 0.01 μm.

The MOUDI data illustrated in Fig. 2 are the averaged results from three replicate measurements with the small error bars representing the standard deviation of the three measurements. The APS data are also averaged results from all of its data collected concurrently with the MOUDI data. The number-based size distribution obtained from the APS show a lognormal distribution with the geometric mean diameter of 0.97 μm and the geometric standard deviation of 1.5. The mass-based size distributions from the MOUDI and the APS are generally in agreement. They both show a bimodal lognormal distribution with a larger mode ~13 μm and another mode <5 μm. The smaller mode is less apparent in the MOUDI data, and it shows lower concentrations compared to the APS data for the dust larger than ~1 μm. These observations most likely result from the loss of larger dusts inside the MOUDI. Larger inertia for the larger dusts may have led to a higher fraction of them bouncing off the substrates where they were supposed to be collected, resulting in a smaller amount of mass collected on the filters. All the size distributions show that a substantial fraction of the airborne dust was respirable (<10 μm). Note that the concentration level shown in Fig. 2 is that monitored in the laboratory setting, which can be very different from those experienced in practice, although the shape of the size distribution is expected to be similar.

Figure 3 shows the size distribution data obtained from the MOUDI for the dust generated from cutting the four fiber cement siding brands. Because three sets of MOUDI samples were collected for cutting each brand, the data points shown in Fig. 3 are the average of the three replicates, and the error bars represent the standard deviations of the corresponding data points. In general, the MOUDI data showed reasonably good repeatability and the dust size distributions are very similar among the four brands. The dust from cutting James Hardie and CertainTeed boards has apparently higher concentration than the other two brands at the size channel of 13.4 μm; and that from cutting James Hardie board has higher concentrations than the other three brands between 4.2 and 7.5 μm, too. All of the data sets show a bimodal lognormal distribution with a larger mode around 13 μm, and another mode between 1 and 3 μm. Combining the size distribution data shown in Fig. 3 and the respirable fraction from the respirable

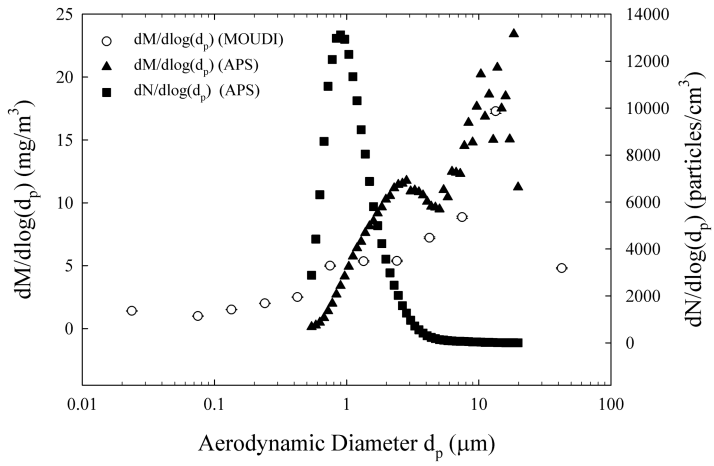

Figure 2 Typical size distribution of the dust from cutting fiber cement siding. Siding: James Hardie.

convention curve, the overall respirable fraction of airborne dust was estimated to be 43.1, 40.9, 48.8, and 37.8% for cutting fiber cement siding from CertainTeed, James Hardie, Maxitile, and Nichiha, respectively.

Dust generation from cutting fiber cement siding of four siding brands

The generation rate (G_{APS} and G_{Cyc}) and the crystalline silica content of the respirable dust for cutting the four siding brands are illustrated in Fig. 4. Each data point is the average obtained from either the three respirable samples collected by the GK4.162 cyclone sampler or the APS data collected simultaneously. The error bars represent the standard deviation of the three replicates.

Compared to the generation rates derived from the APS data (G_{APS}), those obtained from the cyclone sampler (G_{Cyc}) were apparently higher (0.93–1.06 g

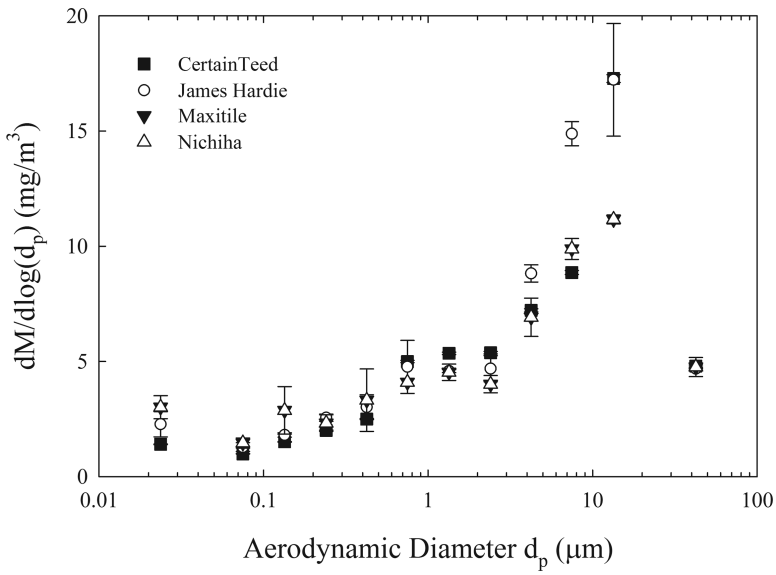

Figure 3 Size distribution obtained from the MOUDI for the dust from cutting fiber cement siding of four siding brands.

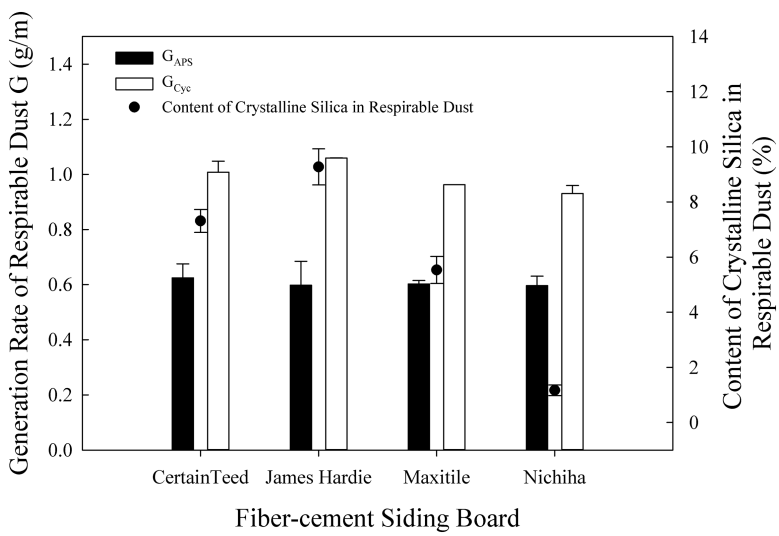

Figure 4 Comparison of the generation rate of respirable dust from cutting fiber cement siding from four siding brands.

m^{-1}). The average of G_{Cyc} was ~63.6% ± 9.3% higher than the average of G_{APS}. Because the cyclone sampler offers a direct gravimetric measurement of the sampled respirable dusts, G_{Cyc} should be considered more representative of the actual generation rates. Volckens and Peters (2005) found that the overall counting efficiency of the APS 3321 was near 100% for solid particles. Thus, the smaller values for G_{APS} might be mainly attributed to possibly underestimated loss of dust in the sampling line and dilutor, as well as the bias introduced by the assumptions that the dust density is equal to the board density, and that all the dusts were spherical. Although the difference between G_{Cyc} and G_{APS} is obvious, this difference is consistent among the four cases shown in Fig. 4. The four pairs of data from Fig. 4 and $G_{Cyc} = G_{APS} = 0$ yield a linear regression equation of $G_{Cyc} = 1.6345 G_{APS} + 0.0006$ with a R^2 of 0.9883. Considering the consistent correlation between G_{Cyc} and G_{APS} and the inclusion of size distribution information in the APS data, using APS alone can be sufficient for tests in the laboratory testing system aiming at comparing the relative dust generation rather than obtaining the actual generation rate under different testing conditions. With the direct reading results and fewer repeated cuts required for the APS, the test can be greatly facilitated.

The results in Fig. 4 also suggest that the respirable dust generation rate for the four siding brands are very close to each other, with a maximum difference of 13.8% for G_{Cyc} and 5.9% for G_{APS}. This result is also consistent with the observation in Fig. 3. The content of crystalline silica in respirable dust, however, varied in a relatively wide range of 1.2–9.3%, perhaps due to the varied formulations the four manufacturers used in their respective products that were evaluated in this study. This is also evidenced by the varying silica content in the bulk dust samples from 4.1 to 32.5% for the four brands.

Silica content in the dust of different sizes

As mentioned earlier, the MOUDI samples offered an additional insight on the content of crystalline silica in the dust of different sizes by analyzing the amount of crystalline silica in the dust collected on each stage of the MOUDI. This information is shown in Fig. 5 for the four siding brands. The data for bulk samples and respirable dust samples shown in Fig. 5 were obtained by analyzing the silica content in the bulk samples and the respirable dust samples. For all four brands, the silica content in the airborne dust showed the same obvious trend of an increase with the aerodynamic diameter of the dust, approaching to the silica content levels found in their respective bulk samples. Each data point is a ratio of the quartz mass over the dust mass. Thus, the error bars shown in Fig. 5 represent the propagated measurement uncertainty calculated from the standard deviations of the quartz and dust measurements following the procedure by Qi and Kulkarni (2013).

The overall trend observed in Fig. 5 is consistent with that in Fig. 4, with the dusts from James Hardie's board containing the highest silica content and those from Nichiha containing the lowest silica content. The results observed for the bulk samples confirm that the difference is due to the different amount of silica used for the respective product. The results in Fig. 5 clearly show that larger dusts contain higher percentage of crystalline silica. This explains why the silica content in the respirable dust samples was considerably lower than in their respective bulk samples. It also supports similar observations by Sirianni *et al.* (2008) and Shepherd *et al.* (2009). This finding is encouraging from the perspective of lowering workers' exposure to RCS as the larger dusts that contain higher percentages of silica are less respirable. It should be noted that the trend of higher silica content in larger dusts shown in Fig. 5 could be partially attributed to the increasing XRD intensity with particle size. A study by Chen *et al.* (2014) found that the XRD analyses for crystalline silica was sensitive to the particle size, with the XRD intensity increasing with the mass median aerodynamic diameters of the dusts. Following the same approach by Chen *et al.* (2014), the silica content for the dust on each stage of the MOUDI was adjusted for the measured XRD intensity. The adjusted data are plotted in Supplementary Fig. S1, and the same trend of higher silica content in larger dusts as shown in Fig. 5 is still observed.

The MOUDI data, including the dust size distribution and silica distribution in the dust of varying sizes, can also be used to derive the overall silica content in the respirable dust with the knowledge of a respirable fraction based on the convention curve for the aerodynamic diameters of the size channels in MOUDI. Supplementary Fig. S2 compares the silica contents in the respirable dusts derived from the MOUDI data

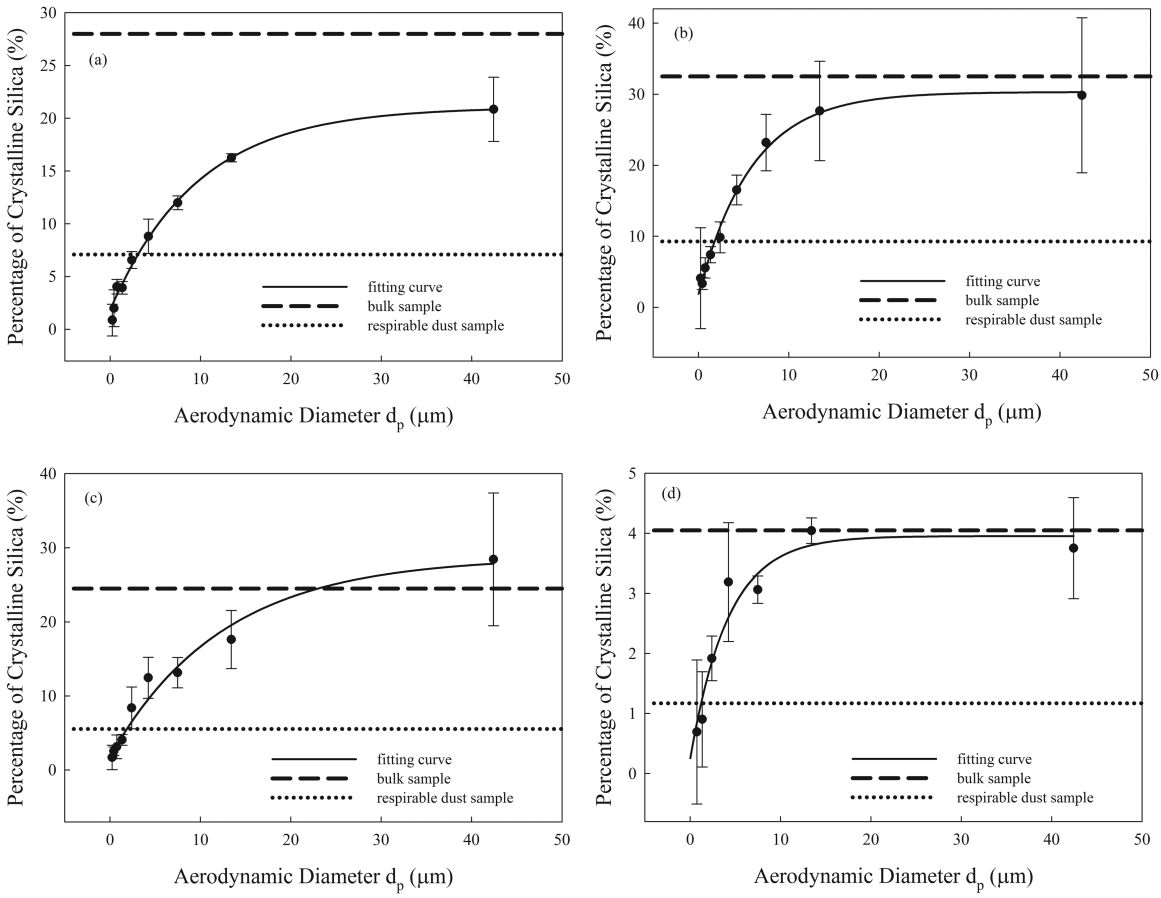

Figure 5 Silica distribution in the dusts of different sizes from cutting fiber cement siding board of (a) CertainTeed; (b) James Hardie; (c) Maxitile; (d) Nichiha.

and obtained from the laboratory respirable dust samples. The results from the two methods are reasonably comparable, with those from the MOUDI data consistently lower than those from the laboratory respirable dust samples (ranging from 0.9 to 6.9% compared to ranging from 1.2 to 9.3%). This is possibly due to the low sizing resolution of the MOUDI and the higher fraction of larger dusts, which contain higher percentage of silica, bouncing off the substrates in the MOUDI.

By combining the results of the dust size distribution from the APS data, respirable fraction from the convention curve, and the silica distribution in the dust of different sizes (fitting curves in Fig. 5), a size distribution of RCS for the dust from cutting fiber cement siding can be estimated for the four brands and are presented in Fig. 6. Most respirable silica resides in the dust ~2.5 μm in aerodynamic diameter, although the overall concentration level varied among the four brands. According to the data shown in Fig. 6, particles >1.0 μm contain about 95% of the RCS. This information can be used to estimate how much RCS would be removed for a specific dust control measure with the knowledge of its capturing efficiency of particles of different sizes.

CONCLUSIONS

Laboratory tests of cutting fiber cement siding in a newly developed laboratory testing system verified that the system provided high repeatability, making it suitable for the targeted characterization of the dust generation rate and size-dependent silica content. Combining the results for both the dust size distribution and size-dependent silica content, it was found that most RCS from cutting fiber cement siding of the four brands resides in the dust ~2.5 μm in aerodynamic diameter. These results would help guide the development of

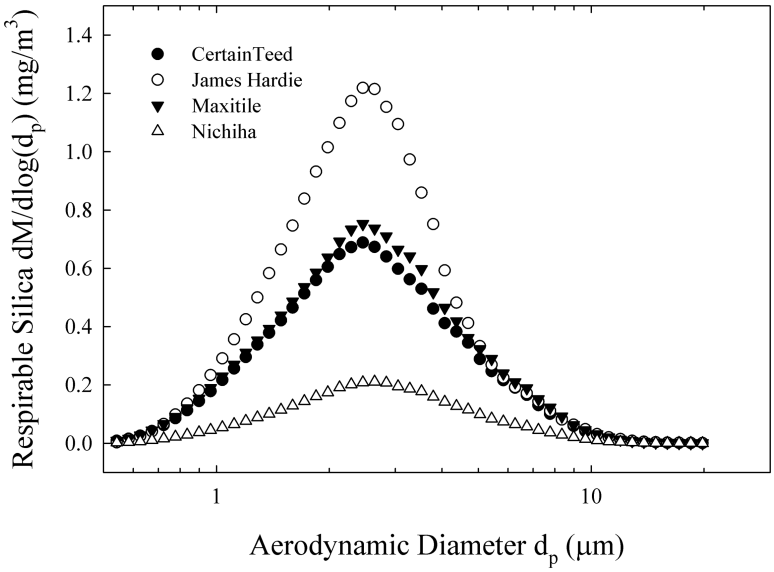

Figure 6 Size distribution of RCS for the dust from cutting fiber cement siding of four siding brands.

specific engineering control measures targeting at lowering workers' exposure to RCS while cutting fiber cement siding. The consistent correlation between the APS data and those from the cyclone and the MOUDI samplers allowed us to use the APS alone in this laboratory testing system and carry out additional tests aiming at comparing the dust generation under different testing conditions, including the deployment of various engineering control measures. A simple and low cost engineering control measure was identified from the laboratory test and later validated from a series of field trials. These results will be published separately. Beyond the current study, this system can also be easily modified to test other types of equipment and materials for the dust generation rate, with a designated fixture holding the testing equipment and an adaptor holding the testing material if needed. A similar approach in this study can then be used to explore the dust generation characteristics and appropriate engineering control solutions for those equipment and materials.

SUPPLEMENTARY DATA

Supplementary data can be found at http://annhyg.oxfordjournals.org/.

FUNDING

National Institute for Occupational Safety and Health project [Partnering to Control Dust from Fiber-Cement Siding (CAN# 0927ZJSB)].

DISCLAIMER

The findings and conclusions in this report are those of the authors and do not necessarily represent the views of the National Institute for Occupational Safety and Health. Mention of product or company name does not constitute endorsement by the Centers for Disease Control and Prevention or NIOSH.

REFERENCES

Brockmann JE. (2011) Aerosol transport in sampling lines and inlets. In Kulkarni P, Baron PA, Willeke K, editors. *Aerosol measurement-principles, techniques, and application*. Hoboken, NJ: John Wiley & Sons. pp. 69–105.

Bureau of Mines. (1992) *Crystalline silica primer*. Washington, DC: U.S. Department of the Interior, Bureau of Mines, Branch of Industrial Minerals, Special Publication.

CEN. (1993) *Centre European de Normalisation Workplace atmospheres: Size fraction definitions for measurement of airborne particles in the workplace, EN 481*. Brussels, Belgium: CEN.

CEN. (2006) *Safety of machinery-Evaluation of the emission of airborne hazardous substances-Part 3: Test bench method for measurement of the emission rate for a given pollutant, EN 1093-3*. Brussels: Belgium: CEN.

Chen CH, Soo JC, Young LH *et al*. (2014) Effect of the quartz particle size on XRD quantifications and its implications for field collected samples. *Aerosol Air Qual Res*; 14: 1573–83.

Health and Safety Laboratory. (2011) *Evaluation of the penetration characteristics of a high flow rate personal cyclone sampler for NIOSH*. By Thorpe A. Derbyshire, UK: Health and Safety Laboratory, Occupational Hygiene Unit.

HSL Contract report prepared for NIOSH, Job Number PE01355.

Heitbrink W, Bennett J. (2006) A numerical and experimental investigation of crystalline silica exposure control during tuck pointing. *J Occup Environ Hyg*; 3: 366–78.

ISO 7708. (1995) *International Organization for Standardization (ISO) 7708 Particle size definitions for health related sampling*. Geneva, Switzerland: ISO.

Lofgren DJ, Johnson DC, Walley TL. (2004) OSHA compliance issues: silica and noise exposure during installation of fiber-cement siding. *J Occup Environ Hyg*; 1: D1–6.

Marple VA, Rubow KL, Behm SM. (1991) A microorifice uniform deposit impactor (MOUDI): description, calibration, and use. *Aerosol Sci Technol*; 14: 434–46.

Mid-West Instrument. (2004) *Delta-tube: application and system design data*. Sterling Heights, MI: Mid-West Instruments, Bulletin No. ASDE/04. Available at http://www.midwestinstrument.com/pdfs/bulletins/DeltaTubeBulletinNo.ASDE04.pdf. Accessed 14 September 2015.

Miller RW. (1989) *Flow measurement engineering handbook*. 2nd edn. New York, NY; McGraw-Hill.

NIOSH. (1986) *Occupational respiratory diseases*. Publication No. 86–102; Cincinnati, OH: National Institute for Occupational Safety and Health.

NIOSH. (1998) *NIOSH manual of analytical methods (NMAM). Particulates not otherwise regulated, respirable, Method 0600, Issue 3*; Cincinnati, OH: National Institute for Occupational Safety and Health.

NIOSH. (2002) *NIOSH hazard review: health effects of occupational exposure to respirable crystalline silica*. Publication No. 2002–129; Cincinnati, OH: National Institute for Occupational Safety and Health.

NIOSH. (2003) *NIOSH manual of analytical methods (NMAM). Silica, crystalline, by XRD (filter redeposition), Method 7500, Issue 4*; Cincinnati, OH: National Institute for Occupational Safety and Health.

Qi C, Echt A, See M. (2013) *In-depth survey report: partnering to control dust from fiber-cement siding*. Cincinnati, OH: DHHS/CDC/NIOSH. Report No. EPHB 358-11a. Available at http://www.cdc.gov/niosh/surveyreports/pdfs/358-11a.pdf. Accessed 14 September 2015.

Qi C, Kulkarni P. (2013) Miniature dual-corona ionizer for bipolar charging of aerosol. *Aerosol Sci Technol*; 47: 81–92.

Shepherd S, Woskie SR, Holcroft C *et al.* (2009) Reducing silica and dust exposures in construction during use of powered concrete-cutting hand tools: efficacy of local exhaust ventilation on hammer drills. *J Occup Environ Hyg*; 6: 42–51.

Sirianni G, Hosgood HD, Slade MD *et al.* (2008) Particle size distribution and particle size-related crystalline silica content in granite quarry dust. *J Occup Environ Hyg*; 5: 279–85.

US Census Bureau. (2013) Survey of Construction, Principle Type of Exterior Wall Material of New One-Family Houses Completed.

Vincent JH. (2007) *Aerosol sampling*. Chichester, UK: John Wiley & Sons. pp. 203.

Volckens J, Peters TM. (2005) Counting and particle transmission efficiency of the aerodynamic particle sizer. *J Aerosol Sci*; 36: 1400–8.